Macroscopic Quantum Superposition in Cavity Optomechanics

Jie-Qiao Liao* and Lin Tian†
School of Natural Sciences, University of California, Merced, California 95343, USA
(Received 23 August 2015; published 19 April 2016)

Quantum superposition in mechanical systems is not only key evidence for macroscopic quantum coherence, but can also be utilized in modern quantum technology. Here we propose an efficient approach for creating macroscopically distinct mechanical superposition states in a two-mode optomechanical system. Photon hopping between the two cavity modes is modulated sinusoidally. The modulated photon tunneling enables an ultrastrong radiation-pressure force acting on the mechanical resonator, and hence significantly increases the mechanical displacement induced by a single photon. We study systematically the generation of the Yurke-Stoler-like states in the presence of system dissipations. We also discuss the experimental implementation of this scheme.

DOI: 10.1103/PhysRevLett.116.163602

Introduction.—Quantum superposition [1] is at the heart of quantum theory and is often considered a signature to distinguish the quantum from the classical world. To date, quantum superposition has been observed in various physical systems [2], such as electronic [3–5], photonic [6–9], and atomic or molecular systems [10,11], ranging from microscopic systems to mesoscopic devices. Nevertheless, it would be desirable to observe quantum superposition in macroscopic mechanical systems with up to 10^{10} atoms [12]. It can help us understand the fundamentals of quantum theory [13], such as quantum decoherence and quantum-classical boundary in the presence of gravity [14], and has wide applications in quantum information processing with continuous variables [9].

Recent advances in microfabrication provide the possibility of producing high-Q mechanical resonators [15]. This progress paves the way for observing and utilizing quantum effects in macrosized mechanical systems [16–23]. Great efforts have been devoted to controlling the mechanical motion in optomechanics [24–26] and nanomechanics [27,28]. However, it remains a challenge to generate macroscopically distinct superposition states [29] in mechanical resonators [30–39]. Decoherence by quantum and thermal fluctuations can often destroy such superposition. Moreover, the natural mechanical displacement induced by a single photon in optomechanical systems is proportional to the ratio of the coupling rate to the mechanical frequency [32], g_0/ω_M [cf. Eq. (1)], which is of the order of 10^{-5}–10^{-2} in realistic systems [26]. To distinguish the single-photon mechanical displacement from its zero-point fluctuation, the ultrastrong coupling condition $g_0 > \omega_M$ needs to be satisfied [32].

In this Letter, we propose an efficient approach for creating superposition of large-amplitude coherent states in a two-mode optomechanical system by introducing a sinusoidally modulated photon hopping between the two cavities. This modulated photon tunneling induces a near-resonant radiation-pressure force acting on the mechanical resonator, with an effective detuning much smaller than the original mechanical frequency, and hence increases the mechanical displacement generated by a single photon. One merit of this method is that the fidelities of the generated mechanical states are not affected by the decay of cavity photons. This feature enables the possibility to observe distinct mechanical superposition states in practical systems.

System.—Consider a two-mode optomechanical system that consists of a free (left) cavity coupled to an optomechanical (right) cavity via a modulated photon-hopping interaction. The system is described by the Hamiltonian ($\hbar = 1$)

$$\hat{H}(t) = \omega_c(\hat{a}_L^\dagger\hat{a}_L + \hat{a}_R^\dagger\hat{a}_R) - \xi\omega_0\cos(\omega_0 t)(\hat{a}_L^\dagger\hat{a}_R + \hat{a}_R^\dagger\hat{a}_L) + \omega_M\hat{b}^\dagger\hat{b} - g_0\hat{a}_R^\dagger\hat{a}_R(\hat{b} + \hat{b}^\dagger), \quad (1)$$

where $\hat{a}_{L(R)}$ and $\hat{b}$ are the annihilation operators of the left (right) cavity mode and the mechanical mode, with resonant frequencies ω_c and ω_M, respectively. The parameter ω_0 is the modulation frequency and ξ is the dimensionless modulation amplitude of photon hopping between the two cavities. g_0 is the magnitude of the single-photon optomechanical coupling between the right cavity and the mechanical mode. Similar two-mode optomechanical systems have been proposed for studying quantum optics and quantum information missions [40–44].

In a rotating frame defined by the transformation operator $\hat{T}(t)=\hat{V}_1(t)\hat{V}_2(t)$, with $\hat{V}_1(t)=\exp\{-i[\omega_c(\hat{a}_L^\dagger\hat{a}_L+\hat{a}_R^\dagger\hat{a}_R)+\omega_M\hat{b}^\dagger\hat{b}]t\}$ and $\hat{V}_2(t) = \exp[i\xi\sin(\omega_0 t)(\hat{a}_L^\dagger\hat{a}_R + \hat{a}_R^\dagger\hat{a}_L)]$, and under the condition $|\delta|, g_0/2 \ll \omega_0, \omega_M$, we can obtain an effective Hamiltonian by the rotating-wave approximation (RWA) as [45]

$$\hat{H}_{\mathrm{RWA}}(t) = g(\hat{a}_L^\dagger\hat{a}_L - \hat{a}_R^\dagger\hat{a}_R)(\hat{b}e^{-i\delta t} + \hat{b}^\dagger e^{i\delta t}). \quad (2)$$

Here, $g = g_0 J_{2n_0}(2\xi)/2$ is the normalized coupling constant under a selected integer n_0 and $\delta = \omega_M - 2n_0\omega_0$ is a modulation-induced detuning, where $J_n(z)$ is the Bessel function of the first kind, and n_0 corresponds to the near-resonance term in the Jacobi-Anger expansions of the sinusoidal factor in $\hat{V}_2(t)$.

The Hamiltonian Eq. (2) describes a driven harmonic oscillator with an effective driving force $g\langle(\hat{a}_L^\dagger \hat{a}_L - \hat{a}_R^\dagger \hat{a}_R)\rangle$ on a mechanical quadrature that rotates at a frequency δ. Under this form, the maximum mechanical displacement induced by a single photon is $2g/|\delta|$, which, by choosing proper ξ and δ, could be much larger than the displacement $2g_0/\omega_M$ [32] in the single-cavity case. The resonance driving effect can be seen more clearly by introducing the symmetric and asymmetric modes of the two cavities [45]: $\hat{a}_\pm = (\hat{a}_L \pm \hat{a}_R)/\sqrt{2}$. In the representation of $\hat{a}_\pm$, the frequencies of modes $\hat{a}_\pm$ are modulated by periodic functions with frequency ω_0, and hence the Floquet sideband modes (with frequencies $\omega_c + m\omega_0$ for integers m) will assist the transitions of the system. As a result, we can choose a proper ω_0 such that the conditional displacement process becomes resonant or near resonant and other processes are far off resonant. The physical picture can also be understood in the time domain [45]. By hopping a single photon into and out of the right cavity at the proper time, the mechanical effect of the single photon will be amplified because the displacement effect can be accumulated when the driving force and the mechanical oscillation are in phase. At the same time, modulation sidebands are designed to suppress other parametric processes, and hence an enhanced radiation-pressure interaction can be obtained.

Generation of Yurke-Stoler-like states.—To generate mechanical superposition states, we consider an initial state $|\psi(0)\rangle = \frac{1}{\sqrt{2}}(|1\rangle_L|0\rangle_R + |0\rangle_L|1\rangle_R)|0\rangle_M$, where $|n = 0, 1\rangle_{L(R)}$ are cavity-field Fock states and $|0\rangle_M$ is the mechanical ground state prepared via ground state cooling [20–22]. Applying the propagator associated with $\hat{H}_{\mathrm{RWA}}(t)$ on this initial state, followed by the transformation $\hat{T}(t)$, we derive the state

$$|\psi(t)\rangle = \frac{e^{i\vartheta}}{\sqrt{2}}[|1\rangle_L|0\rangle_R|\varphi_L(t)\rangle_M + |0\rangle_L|1\rangle_R|\varphi_R(t)\rangle_M], \quad (3)$$

where $\vartheta(t) = -(\omega_c - g^2/\delta)t - (g^2/\delta^2)\sin(\delta t)$ is a global phase factor. The two states $|\varphi_L(t)\rangle_M = \cos(\mu/2)|\beta(t)\rangle_M + i\sin(\mu/2)|-\beta(t)\rangle_M$ and $|\varphi_R(t)\rangle_M = (|\varphi_L(t)\rangle_M)|_{\beta\leftrightarrow-\beta}$ are Yurke-Stoler-like states [58], which are quantum superposition of coherent states $|\pm\beta(t)\rangle_M$, where $\beta(t) = [-2ig\sin(\delta t/2)/\delta]e^{-i(\omega_M-\delta/2)t}$ and $\mu(t) = 2\xi\sin(\omega_0 t)$. For the resonant case $\delta = 0$, we have $\beta_{\mathrm{res}}(t) = -igt\exp(-i\omega_M t)$. Equation (3) describes a three-mode entangled state that involves two cavity modes and a mechanical mode. To generate mechanical superposition states $|\varphi_{L(R)}(t)\rangle_M$, we need to measure the states of the cavity field.

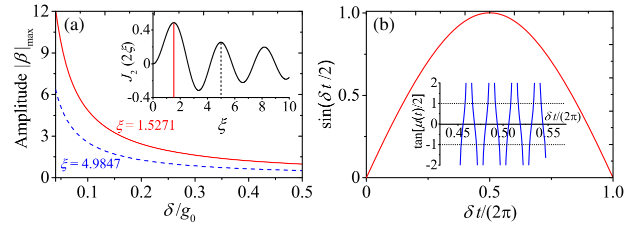

FIG. 1. (a) The maximum amplitude $|\beta|_{\max}$ vs δ/g_0 at $\xi = 1.5271$ and 4.9847, which correspond to the peak values of the Bessel function $J_2(2\xi)$, as shown in the inset. (b) Time dependence of $\sin(\delta t/2)$ and $\tan[\mu(t)/2]$ near the positions that give the large oscillation amplitude and the equal probability superposition in states $|\varphi_{L(R)}(t)\rangle_M$, where $\omega_M/\delta = 80$, $n_0 = 1$, and $\xi = 1.527$.

The maximum coherent amplitude, $|\beta|_{\max} = 2g/\delta$, is controllable by tuning the two parameters ξ and ω_0 based on the relations $g = g_0 J_{2n_0}(2\xi)/2$ and $\delta = \omega_M - 2n_0\omega_0$. We choose proper n_0 and optimal ξ to reach peak values of the Bessel function $J_{2n_0}(2\xi)$, and tune the modulation frequency ω_0 such that the value of δ can be changed continuously. In Fig. 1(a), we plot $|\beta|_{\max}$ as a function of δ when the first two peak values of $J_2(2\xi)$ (with $n_0 = 1$) are taken (inset). A macroscopically distinct coherent amplitude can always be obtained by choosing $\delta < 2g$ such that $|\beta|_{\max} > 1$ and then $|\langle-\beta|\beta\rangle| \ll 1$. In this case, the two coherent states become approximately distinguishable in phase space by proper quadrature measurements [58,59].

The amplitude $|\beta| = (2g/\delta)|\sin(\delta t/2)|$ reaches its maximum values at times $t_m = (2m+1)\pi/\delta$ [i.e., $\sin(\delta t_m/2) = \pm 1$] for non-negative integers m. Meanwhile, the relative probability amplitudes of the states $|\varphi_{L(R)}(t)\rangle_M$ depend on the time through $\mu(t)$. To observe strong evidence of quantum interference, one expects that the two components $|\pm\beta(t)\rangle_M$ appear with comparable probabilities. This leads to $\mu(\tau_n) = 2\xi\sin(\omega_0\tau_n) \approx (n + 1/2)\pi$ [i.e., $\tan[\mu(\tau_n)/2] \approx \pm 1$] for non-negative integers n. Near a given value of t_m, there are many τ_n satisfying the probability requirement because of $\omega_0 \gg \delta$. Hence, we can choose proper time windows τ_n such that $|\beta(\tau_n)| > 1$. In Fig. 1(b), we plot the function $\sin(\delta t/2)$ and show the function $\tan[\mu(t)/2]$ around the time $t_0 = \pi/\delta$ (inset). We can see that around t_0 there are many values of time satisfying the two requirements at the same time. In addition, the timing period of the measurement is slower than the periodic oscillation of the mechanical mode because of $\omega_0 \approx \omega_M/2$. In realistic experiments, one can turn off the photon hopping at the detection time t_d (the photon detection time, one of τ_n around t_0), then the evolution of the system can be approximated as a free evolution because the bare optomechanical coupling strength g_0 is much smaller than ω_M. As a result, a wider time window can be obtained for implementing proper measurements for the cavities and the mechanical mode.

The above analyses show a trade-off between the displacement amplitude $|\beta|_{\max} = 2g/\delta$ and the state generation time $t_0 = \pi/\delta$. We pursue a large $|\beta|_{\max}$ for macroscopic superposition and a small t_0 for reducing the impact of the dissipations. In realistic simulations, we should choose a proper δ such that $|\beta|_{\max}$ satisfies the requirement of macroscopicity and t_0 is as small as possible. It is also worth mentioning that the detection time can be shortened by utilizing the upslope rather than the peak of the amplitude function $|\sin(\delta t/2)|$ with a smaller δ. For example, to obtain a displacement of $|\beta|_{\max} = 2$, the time for the resonant case $\delta = 0$ is $t_{\text{res}} = 2/g$, which is shorter than $t_0 = \pi/g$ for the case $\delta = g$ [45].

Effects of dissipations.—To study the environmental fluctuation effects on the state generation scheme, we numerically simulate the state generation in the open system case, in which the evolution of our system is governed by the quantum master equation [45]:

$$\dot{\hat{\rho}} = i[\hat{\rho}, \hat{H}(t)] + \gamma_c \mathcal{D}[\hat{a}_L]\hat{\rho} + \gamma_c \mathcal{D}[\hat{a}_R]\hat{\rho} + \gamma_M (n_{\text{th}} + 1)\mathcal{D}[\hat{b}]\hat{\rho} + \gamma_M n_{\text{th}} \mathcal{D}[\hat{b}^\dagger]\hat{\rho}, \quad (4)$$

where $\mathcal{D}[\hat{o}]\hat{\rho} = \hat{o}\,\hat{\rho}\,\hat{o}^\dagger - (\hat{o}^\dagger\hat{o}\,\hat{\rho} + \hat{\rho}\hat{o}^\dagger\hat{o})/2$ is the standard Lindblad superoperator for photon and phonon dampings, γ_c and γ_M are the damping rates of the cavity fields and the mechanical mode, respectively, and n_{th} is the thermal phonon occupation number. We numerically solve the master equation and calculate the reduced density matrix $\hat{\rho}_M^{(L)}(t)$ $[\hat{\rho}_M^{(R)}(t)]$ of the mechanical mode [45], the probability $P_{L(R)}(t)$ of the photon in the left (right) cavity, and the fidelity $F_{s=L(R)}(t) = {}_M\langle\varphi_s(t)|\hat{\rho}_M^{(s)}(t)|\varphi_s(t)\rangle_M$ between the generated mechanical states and the target states.

In Fig. 2(a), we show the time dependence of the probability $P_L(t)$ at selected values of the cavity-field decay rate γ_c. Note that $P_R(t)$ has a similar pattern to $P_L(t)$ except for a slight oscillation [hereafter, we display only $P_L(t)$ and $F_L(t)$ for concision]. We see that $P_L(t)$ has an approximate exponential decay envelope with the corresponding γ_c and slight oscillations. We also show the probabilities $P_L(t_d)$ and $P_R(t_d)$ at time t_d as a function of γ_c (inset). The curves indicate that $P_{L(R)}(t_d)$ decreases with the increase of γ_c. About the fidelity, our numerical results show that the fidelities $F_L(t)$ and $F_R(t)$ have a similar pattern, and that the fidelities are independent of the decay rate γ_c, as shown in both the dynamics [Fig. 2(b)] and the fidelity at time t_d (inset). Here the negligible difference between $F_L(t_d) = 0.943$ and $F_R(t_d) = 0.939$ is caused by the RWA, and it will disappear gradually with the increase of ω_M/g_0. In the presence of photon dissipation, the photon could leak out of the cavities before the measurement. However, the normalization of the density matrices after the measurement ensures that in the selected experiments the photon remains in the cavities. Hence, the fidelity of the generated state is not affected by photon decay.

To evaluate the quantum coherence and interference effects in the generated superposition states $\hat{\rho}_M^{(L)}(t_d)$ and $\hat{\rho}_M^{(R)}(t_d)$, we examine the Wigner function $W_{s=L(R)}(\eta) = \frac{2}{\pi}\mathrm{Tr}[\hat{D}^\dagger(\eta)\hat{\rho}_M^{(s)}(t_d)\hat{D}(\eta)(-1)^{\hat{b}^\dagger\hat{b}}]$ [60], where $\hat{D}(\eta) = \exp(\eta\hat{b}^\dagger - \eta^*\hat{b})$ is the displacement operator. It can be seen from the relation $|\varphi_R(t_d)\rangle_M = (|\varphi_L(t_d)\rangle_M)|_{\beta\leftrightarrow-\beta}$ that the Wigner function $W_R(\eta)$ should be a rotation of $W_L(\eta)$ by π about the origin in phase space. We perform the simulations with the parameters in Fig. 2 and find that there is also a negligible difference between $W_R(\eta)$ and the π-rotated $W_L(\eta)$. The difference disappears gradually with the increase of ω_M/g_0. We also find that the Wigner functions are independent of the cavity-field decay rate, in accordance with the fidelities. In Fig. 2(c) we display the Wigner function $W_L(\eta)$ of the state $\hat{\rho}_M^{(L)}(t_d)$. We see obvious interference evidence in this Wigner function.

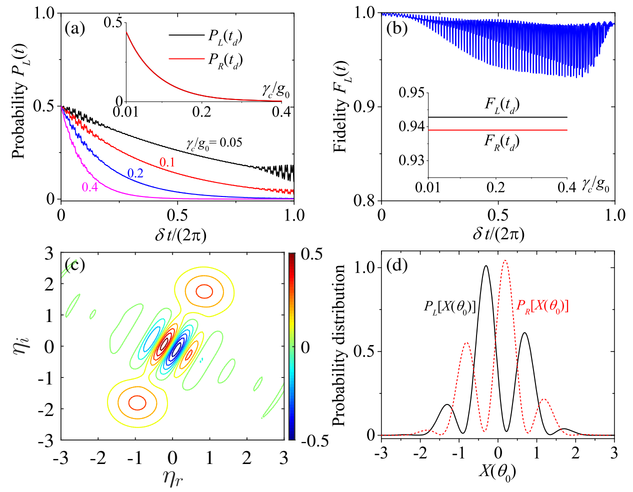

FIG. 2. (a) The probability $P_L(t)$ and (b) the fidelity $F_L(t)$ vs δt at selected values of the cavity-field decay rate γ_c. Insets: The probability $P_{L(R)}(t_d)$ and the fidelity $F_{L(R)}(t_d)$ at time t_d versus γ_c/g_0. (c) The Wigner function $W_L(\eta)$ (with $\eta = \eta_r + i\eta_i$) and (d) the probability distribution of the rotated quadrature operator $P_L[X(\theta_0)]$ for the state $\hat{\rho}_M^{(L)}(t_d)$. Other parameters are $\omega_M/g_0 = 20$, $n_0 = 1$, $\xi = 1.5271$, $\delta = g$, $\gamma_M/g_0 = 0.0001$, and $n_{\text{th}} = 4$.

The quantum superposition properties can also be seen in the probability distribution $P_{s=L(R)}[X(\theta)] = {}_M\langle X(\theta)|\hat{\rho}_M^{(s)}(t_d)|X(\theta)\rangle_M$ of the rotated quadrature operator $\hat{X}(\theta) = (\hat{b}e^{-i\theta} + \hat{b}^\dagger e^{i\theta})/\sqrt{2}$ [61], where $|X(\theta)\rangle_M$ is the eigenstate of $\hat{X}(\theta)$: $\hat{X}(\theta)|X(\theta)\rangle_M = X(\theta)|X(\theta)\rangle_M$. In Fig. 2(d), we plot the probability distributions $P_L[X(\theta_0)]$ and $P_R[X(\theta_0)]$ as functions of $X(\theta_0)$. Here the rotation angle is chosen as $\theta_0 = \arg[\beta(t_d)] - \pi/2$, which means that the quadrature direction is perpendicular to the link line between the locations of the two superposed coherent amplitudes. The interference is maximum in this direction because the two coherent states are projected onto the quadrature such that they overlap exactly. The oscillation in the curves is a distinct evidence of the quantum interference between the superposition components. We notice that $P_L[X(\theta_0)]$ and $P_R[X(\theta_0)]$ are approximately symmetric to each other about the vertical axis $X(\theta_0) = 0$, in

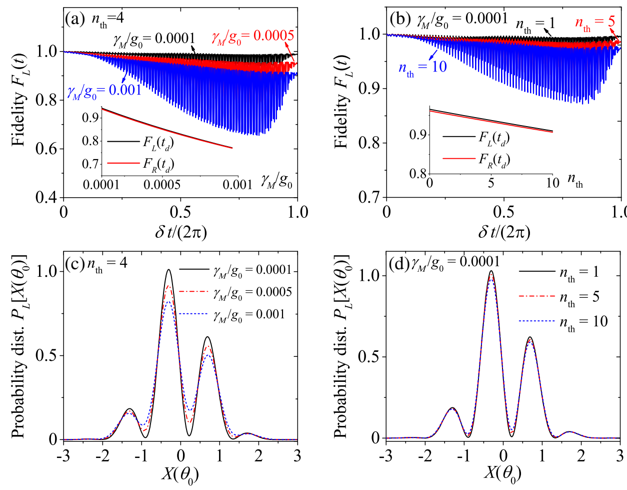

FIG. 3. The fidelity $F_L(t)$ vs δt at selected values of (a) the mechanical decay rate γ_M/g_0 and (b) the thermal phonon occupation number $n_{\rm th}$. Insets: The fidelity $F_{L(R)}(t_d)$ at time t_d vs γ_M/g_0 and $n_{\rm th}$. The probability distribution of the rotated quadrature operator $P_L[X(\theta_0)]$ of the state $\hat{\rho}_M^{(L)}(t_d)$ at selected values of (c) γ_M/g_0 and (d) $n_{\rm th}$. Other parameters are $\omega_M/g_0 = 20$, $n_0 = 1$, $\xi = 1.5271$, $\delta = g$, and $\gamma_c/g_0 = 0.2$.

accordance with the negligible difference between $F_L(t)$ and $F_R(t)$.

We also investigate the influence of mechanical noise on the state generation. Our numerical simulations verify that the probabilities $P_L(t)$ and $P_R(t)$ are independent of γ_M and $n_{\rm th}$. On the contrary, the mechanical dissipations affect the fidelities $F_L(t)$ and $F_R(t)$. In Figs. 3(a) and 3(b), we show the dynamics of the fidelity $F_L(t)$ at selected values of γ_M and $n_{\rm th}$, respectively. We can see $F_L(t)$ becomes worse for larger values of γ_M and $n_{\rm th}$. In addition, the fidelities $F_L(t_d)$ and $F_R(t_d)$ at time t_d decrease with the increase of γ_M and $n_{\rm th}$ (insets). In Figs. 3(c) and 3(d), we plot the probability distribution $P_L[X(\theta_0)]$ for the state $\hat{\rho}_M^{(L)}(t_d)$ with the parameters in Figs. 3(a) and 3(b), respectively [we can know $P_R[X(\theta_0)]$ from the approximate symmetry between $P_L[X(\theta_0)]$ and $P_R[X(\theta_0)]$]. Here we can see that the oscillatory feature of $P_L[X(\theta_0)]$ disappears gradually with the increase of γ_M and $n_{\rm th}$. These results imply that mechanical dissipations will destroy the quantum coherence and interference effects in the generated mechanical superposition. In our simulations, quantum interference evidence can be seen, and good fidelities (> 0.9) can be obtained.

Discussions.—Our state generation approach is general and it can be principally implemented in various optomechanical setups. Below, we focus our discussion on electromechanical systems with cavities in the microwave regime. For such systems, the photon hopping between superconducting resonators can be realized via Josephson junction coupling [62]. The initial Bell state of the cavity fields can be prepared by a superconducting qubit, as realized in circuit-QED systems [63,64]. In particular, a nonperfect photon loading (i.e., containing the zero-photon component) does not affect the fidelity but decreases the success probability of the generated mechanical states because all the couplings will be frozen when there are no photons in the two cavities. The photon states in the superconducting resonators can be measured via superconducting quits [65]. In addition, the generated mechanical superposition states can be measured by the technique of quantum state reconstruction [66–68]. We use another cavity mode (in the same resonator) to build a connection between the mechanical mode and the output field. By detecting the quadrature of the output field, we can obtain the information of the mechanical states [45].

The parameter conditions for implementation of this scheme are $g_0 \ll \omega_M$, the ratio g_0/γ_c should be moderately larger than 1 for a high success probability (for example, $g_0/\gamma_c = 5$–10 corresponds to the success probability 0.08–0.285), and $n_{\rm th} \ll g_0/(4\pi\gamma_M)$. Below, we analyze the conditions in detail [45]. (i) For state generation purposes, we choose $\delta < 2g \ll \omega_M$, then the RWA condition can be simplified as $g_0 \ll \omega_M$, which is consistence with the current experimental situation [26]: g_0/ω_M is of the order of 10^{-5}–10^{-3}. (ii) The photon decay does not affect the fidelity, but it affects the probability by $\mathcal{P} \approx e^{-4\pi\gamma_c/g_0}$ at $\delta = g$. Currently, the value of g_0/γ_c is 10^{-4}–10^{-2} [25]. This value can be increased by either increasing g_0 or decreasing γ_c. In electromechanical systems, $\gamma_c = 2\pi \times 170$ kHz [69] and $\gamma_c = 2\pi \times 118$ kHz [70] have been reported. The value of γ_c can be further decreased to be dozens of kilohertz [71]. The largest value of g_0 reported in electromechanics is $2\pi \times 460$ Hz [69], and theoretic estimations indicate that it can reach megahertz by utilizing the nonlinearity in Josephson junction [72,73]. Therefore, $g_0/\gamma_c > 5$ should be accessible in the near future. In particular, in the resonant case $\delta = 0$ and at $|\beta|_{\max} = 1$, the success probability can be improved to be $\mathcal{P} \approx e^{-4\gamma_c/g_0}$, which takes $\mathcal{P} = 0.14$–0.45 for $g_0/\gamma_c = 2$–5. (iii) The thermal phonon number $n_{\rm th}$ should be small such that the state generation time is much shorter than the characteristic coherence time of the phonons, i.e., $t_d \approx 4\pi/g_0 \ll 1/(\gamma_M n_{\rm th})$, which leads to $n_{\rm th} \ll g_0/(4\pi\gamma_M)$. Currently, the ratio g_0/γ_M is 10^1–10^2 [26] (this value can be increased to 10^4 when g_0 is increased as described above). In a low-temperature environment, $n_{\rm th} < 30$ can be obtained. For example, at $T = 10$ mK [70], we have $n_{\rm th} \approx 20$ at $\omega_M = 2\pi \times 10$ MHz. Therefore, the condition $n_{\rm th} \ll g_0/(4\pi\gamma_M)$ can be satisfied in electromechanics. Based on the above discussions, we suggest the parameters to be $\omega_c = 2\pi \times (5$–$10)$ GHz, $\gamma_c = 2\pi \times (25$–$200)$ kHz, $\omega_M = 2\pi \times 10$ MHz, $\gamma_M = 2\pi \times (50$–$500)$ Hz, and $g_0 = 2\pi \times 500$ kHz, which are consistent with the values used in our simulations [45].

Conclusions.—We have proposed an efficient method for creating macroscopically distinct superposition states in a mechanical resonator. This method is based on the introduction of a modulated photon-hopping interaction in a two-mode optomechanical system to produce large effective single-photon optomechanical coupling. Numerical simulations demonstrate that our method works well in the presence of dissipations and can be realized in a wide parameter range.

The authors are supported by the DARPA ORCHID program through AFOSR and the National Science Foundation under Award No. NSF-DMR-0956064.

*jieqiaoliao@gmail.com
†ltian@ucmerced.edu

[1] P. A. M. Dirac, *The Principles of Quantum Mechanics* (Oxford University Press, Oxford, 1958).
[2] M. Arndt and K. Hornberger, Nat. Phys. **10**, 271 (2014), and references therein.
[3] J. Clarke, A. N. Cleland, M. H. Devoret, D. Esteve, and J. M. Martinis, Science **239**, 992 (1988).
[4] J. R. Friedman, V. Patel, W. Chen, S. K. Tolpygo, and J. E. Lukens, Nature (London) **406**, 43 (2000).
[5] C. H. van der Wal, A. C. J. ter Haar, F. K. Wilhelm, R. N. Schouten, C. J. P. M. Harmans, T. P. Orlando, S. Lloyd, and J. E. Mooij, Science **290**, 773 (2000).
[6] M. Brune, E. Hagley, J. Dreyer, X. Maître, A. Maali, C. Wunderlich, J. M. Raimond, and S. Haroche, Phys. Rev. Lett. **77**, 4887 (1996).
[7] J. S. Neergaard-Nielsen, B. M. Nielsen, C. Hettich, K. Mølmer, and E. S. Polzik, Phys. Rev. Lett. **97**, 083604 (2006).
[8] A. Ourjoumtsev, H. Jeong, R. Tualle-Brouri, and P. Grangier, Nature (London) **448**, 784 (2007).
[9] B. Vlastakis, G. Kirchmair, Z. Leghtas, S. E. Nigg, L. Frunzio, S. M. Girvin, M. Mirrahimi, M. H. Devoret, and R. J. Schoelkopf, Science **342**, 607 (2013).
[10] C. Monroe, D. M. Meekhof, B. E. King, and D. J. Wineland, Science **272**, 1131 (1996).
[11] M. Arndt, O. Nairz, J. Vos-Andreae, C. Keller, G. van der Zouw, and A. Zeilinger, Nature (London) **401**, 680 (1999).
[12] A. J. Leggett, J. Phys. Condens. Matter **14**, R415 (2002).
[13] W. H. Zurek, Phys. Today **44**, No. 10, 36 (1991); arXiv: quant-ph/0306072.
[14] M. P. Blencowe, Phys. Rev. Lett. **111**, 021302 (2013).
[15] K. C. Schwab and M. L. Roukes, Phys. Today **58** (7), 36 (2005).
[16] D. Rugar, R. Budakian, H. J. Mamin, and B. W. Chui, Nature (London) **430**, 329 (2004).
[17] A. Naik, O. Buu, M. D. LaHaye, A. D. Armour, A. A. Clerk, M. P. Blencowe, and K. C. Schwab, Nature (London) **443**, 193 (2006).
[18] C. A. Regal, J. D. Teufel, and K. W. Lehnert, Nat. Phys. **4**, 555 (2008).
[19] A. D. O'Connell, M. Hofheinz, M. Ansmann, R. C. Bialczak, M. Lenander, E. Lucero, M. Neeley, D. Sank, H. Wang, M. Weides, J. Wenner, J. M. Martinis, and A. N. Cleland, Nature (London) **464**, 697 (2010).
[20] J. D. Teufel, T. Donner, D. Li, J. W. Harlow, M. S. Allman, K. Cicak, A. J. Sirois, J. D. Whittaker, K. W. Lehnert, and R. W. Simmonds, Nature (London) **475**, 359 (2011).
[21] J. Chan, T. P. Mayer Alegre, A. H. Safavi-Naeini, J. T. Hill, A. Krause, S. Gröblacher, M. Aspelmeyer, and O. Painter, Nature (London) **478**, 89 (2011).
[22] E. Verhagen, S. Deléglise, S. Weis, A. Schliesser, and T. J. Kippenberg, Nature (London) **482**, 63 (2012).
[23] S. Kolkowitz, A. C. Bleszynski Jayich, Q. P. Unterreithmeier, S. D. Bennett, P. Rabl, J. G. E. Harris, and M. D. Lukin, Science **335**, 1603 (2012).
[24] T. J. Kippenberg and K. J. Vahala, Science **321**, 1172 (2008).
[25] M. Aspelmeyer, P. Meystre, and K. Schwab, Phys. Today **65** (7), 29 (2012).
[26] M. Aspelmeyer, T. J. Kippenberg, and F. Marquardt, Rev. Mod. Phys. **86**, 1391 (2014).
[27] M. Blencowe, Phys. Rep. **395**, 159 (2004).
[28] M. Poot and H. S. J. van der Zant, Phys. Rep. **511**, 273 (2012).
[29] S. Nimmrichter and K. Hornberger, Phys. Rev. Lett. **110**, 160403 (2013).
[30] S. Bose, K. Jacobs, and P. L. Knight, Phys. Rev. A **59**, 3204 (1999).
[31] A. D. Armour, M. P. Blencowe, and K. C. Schwab, Phys. Rev. Lett. **88**, 148301 (2002).
[32] W. Marshall, C. Simon, R. Penrose, and D. Bouwmeester, Phys. Rev. Lett. **91**, 130401 (2003).
[33] L. Tian, Phys. Rev. B **72**, 195411 (2005).
[34] O. Romero-Isart, A. C. Pflanzer, F. Blaser, R. Kaltenbaek, N. Kiesel, M. Aspelmeyer, and J. I. Cirac, Phys. Rev. Lett. **107**, 020405 (2011).
[35] B. Pepper, R. Ghobadi, E. Jeffrey, C. Simon, and D. Bouwmeester, Phys. Rev. Lett. **109**, 023601 (2012).
[36] H. Tan, F. Bariani, G. Li, and P. Meystre, Phys. Rev. A **88**, 023817 (2013).
[37] U. Akram, W. P. Bowen, and G. J. Milburn, New J. Phys. **15**, 093007 (2013).
[38] W. Ge and M. S. Zubairy, Phys. Rev. A **91**, 013842 (2015).
[39] J.-Q. Liao, C. K. Law, L.-M. Kuang, and F. Nori, Phys. Rev. A **92**, 013822 (2015).
[40] H. Miao, S. Danilishin, T. Corbitt, and Y. Chen, Phys. Rev. Lett. **103**, 100402 (2009).
[41] J. M. Dobrindt and T. J. Kippenberg, Phys. Rev. Lett. **104**, 033901 (2010).
[42] M. Ludwig, A. H. Safavi-Naeini, O. Painter, and F. Marquardt, Phys. Rev. Lett. **109**, 063601 (2012).
[43] K. Stannigel, P. Komar, S. J. M. Habraken, S. D. Bennett, M. D. Lukin, P. Zoller, and P. Rabl, Phys. Rev. Lett. **109**, 013603 (2012).
[44] P. Kómár, S. D. Bennett, K. Stannigel, S. J. M. Habraken, P. Rabl, P. Zoller, and M. D. Lukin, Phys. Rev. A **87**, 013839 (2013).
[45] See Supplemental Material at http://link.aps.org/supplemental/10.1103/PhysRevLett.116.163602, which includes Refs. [46–57], for the derivation of the effective Hamiltonians, the physical explanation, the detailed calculations in the closed- and open-system cases, and the discussions on physical implementation.
[46] F. A. M. de Oliveira, M. S. Kim, P. L. Knight, and V. Buzek, Phys. Rev. A **41**, 2645 (1990).
[47] T. Rocheleau, T. Ndukum, C. Macklin, J. B. Hertzberg, A. A. Clerk, and K. C. Schwab, Nature (London) **463**, 72 (2010).

[48] J. B. Hertzberg, T. Rocheleau, T. Ndukum, M. Savva, A. A. Clerk, and K. C. Schwab, Nat. Phys. **6**, 213 (2010).
[49] T. A. Palomaki, J. D. Teufel, R. W. Simmonds, and K. W. Lehnert, Science **342**, 710 (2013).
[50] T. A. Palomaki, J. W. Harlow, J. D. Teufel, R. W. Simmonds, and K. W. Lehnert, Nature (London) **495**, 210 (2013).
[51] E. E. Wollman, C. U. Lei, A. J. Weinstein, J. Suh, A. Kronwald, F. Marquardt, A. A. Clerk, and K. C. Schwab, Science **349**, 952 (2015).
[52] J.-M. Pirkkalainen, E. Damskägg, M. Brandt, F. Massel, and M. A. Sillanpää, Phys. Rev. Lett. **115**, 243601 (2015).
[53] F. Lecocq, J. B. Clark, R. W. Simmonds, J. Aumentado, and J. D. Teufel, Phys. Rev. Lett. **116**, 043601 (2016).
[54] P. Rabl, Phys. Rev. Lett. **107**, 063601 (2011).
[55] J.-Q. Liao and C. K. Law, Phys. Rev. A **87**, 043809 (2013).
[56] A. Nunnenkamp, K. Børkje, and S. M. Girvin, Phys. Rev. Lett. **107**, 063602 (2011).
[57] J.-Q. Liao, H. K. Cheung, and C. K. Law, Phys. Rev. A **85**, 025803 (2012).
[58] B. Yurke and D. Stoler, Phys. Rev. Lett. **57**, 13 (1986).
[59] G. Björk and P. G. Luca Mana, J. Opt. B **6**, 429 (2004).
[60] S. M. Barnett and P. M. Radmore, *Methods in Theoretical Quantum Optics* (Clarendon Press, Oxford, 1997).
[61] D. F. Walls and G. J. Milburn, *Quantum Optics* (Springer, Berlin, 2008).
[62] M. H. Devoret, in *Quantum Fluctuations*, edited by S. Reynaud, E. Giacobino, and J. Zinn-Justin (Elsevier, Amsterdam, 1997).
[63] M. Hofheinz, E. M. Weig, M. Ansmann, R. C. Bialczak, E. Lucero, M. Neeley, A. D. O'Connell, H. Wang, J. M. Martinis, and A. N. Cleland, Nature (London) **454**, 310 (2008).
[64] M. Hofheinz, H. Wang, M. Ansmann, R. C. Bialczak, E. Lucero, M. Neeley, A. D. O'Connell, D. Sank, J. Wenner, J. M. Martinis, and A. N. Cleland, Nature (London) **459**, 546 (2009).
[65] D. I. Schuster, A. A. Houck, J. A. Schreier, A. Wallraff, J. M. Gambetta, A. Blais, L. Frunzio, J. Majer, B. Johnson, M. H. Devoret, S. M. Girvin, and R. J. Schoelkopf, Nature (London) **445**, 515 (2007).
[66] D. Vitali, S. Gigan, A. Ferreira, H. R. Böhm, P. Tombesi, A. Guerreiro, V. Vedral, A. Zeilinger, and M. Aspelmeyer, Phys. Rev. Lett. **98**, 030405 (2007).
[67] X.-Y. Lü, J.-Q. Liao, L. Tian, and F. Nori, Phys. Rev. A **91**, 013834 (2015).
[68] M. R. Vanner, I. Pikovski, and M. S. Kim, Ann. Phys. (Berlin) **527**, 15 (2015).
[69] J. D. Teufel, D. Li, M. S. Allman, K. Cicak, A. J. Sirois, J. D. Whittaker, and R. W. Simmonds, Nature (London) **471**, 204 (2011).
[70] L. D. Tóth, N. R. Bernier, A. Nunnenkamp, E. Glushkov, A. K. Feofanov, and T. J. Kippenberg, arXiv:1602.05180.
[71] A. Megrant, C. Neill, R. Barends, B. Chiaro, Y. Chen, L. Feigl, J. Kelly, E. Lucero, M. Mariantoni, P. J. J. OMalley, D. Sank, A. Vainsencher, J. Wenner, T. C. White, Y. Yin, J. Zhao, C. J. Palmstrøm, J. M. Martinis, and A. N. Cleland, Appl. Phys. Lett. **100**, 113510 (2012).
[72] A. J. Rimberg, M. P. Blencowe, A. D. Armour, and P. D. Nation, New J. Phys. **16**, 055008 (2014).
[73] T. T. Heikkilä, F. Massel, J. Tuorila, R. Khan, and M. A. Sillanpää, Phys. Rev. Lett. **112**, 203603 (2014).